Inorg. Chem. **2004**, *43*, 812–821

Syntheses, Luminescence Behavior, and Assembly Reaction of Tetraalkynylplatinate(II) Complexes: Crystal Structures of $[Pt(^tBu_3trpy)(C{\equiv}CC_5H_4N)Pt(^tBu_3trpy)](PF_6)_3$ and $[Pt_2Ag_4(C{\equiv}CC{\equiv}CC_6H_4CH_3\text{-}4)_8(THF)_4]$

Vivian Wing-Wah Yam,* Chi-Kuen Hui, Shu-Yan Yu, and Nianyong Zhu

Center for Carbon-Rich Molecular and Nanoscale Metal-Based Materials Research and Department of Chemistry, The University of Hong Kong, Pokfulam Road, Hong Kong, People's Republic of China

Received July 25, 2003

A series of tetraalkynylplatinate(II) complexes, $(NBu_4)_2[Pt(C{\equiv}CR)_4]$ (R = C_6H_4N-4, C_6H_4N-3, and $C_6H_3N_2$-5), and the diynyl analogues, $(NBu_4)_2[Pt(C{\equiv}CC{\equiv}CR)_4]$ (R = C_6H_5 and $C_6H_4CH_3$-4), have been synthesized. These complexes displayed intense photoluminescence, which was assigned as metal-to-ligand charge transfer (MLCT) transitions. Reaction of $(Bu_4N)_2[Pt(C{\equiv}CC_5H_4N\text{-}4)_4]$ with 4 equiv of $[Pt(^tBu_3trpy)(MeCN)](OTf)_2$ in methanol did not yield the expected pentanuclear platinum product, $[Pt(C{\equiv}CC_5H_4N)_4\{Pt(^tBu_3trpy)\}_4](OTf)_6$, but instead afforded a strongly luminescent 4-ethynylpyridine-bridged dinuclear complex, $[Pt(^tBu_3trpy)(C{\equiv}CC_5H_4N)Pt(^tBu_3trpy)](PF_6)_3$, which has been structurally characterized. The emission origin is assigned as derived from states of predominantly ^{3}MLCT [$d_\pi(Pt) \rightarrow \pi^*(^tBu_3trpy)$] character, probably mixed with some intraligand ^{3}IL [$\pi \rightarrow \pi^*(C{\equiv}C)$], and ligand-to-ligand charge transfer ^{3}LLCT [$\pi(C{\equiv}C) \rightarrow \pi^*(^tBu_3trpy)$] character. On the other hand, reaction of $(Bu_4N)_2[Pt(C{\equiv}CC{\equiv}CC_6H_4CH_3\text{-}4)_4]$ with $[Ag(MeCN)_4][BF_4]$ gave a mixed-metal aggregate, $[Pt_2Ag_4(C{\equiv}CC{\equiv}CC_6H_4CH_3\text{-}4)_8(THF)_4]$. The crystal structure of $[Pt_2Ag_4(C{\equiv}CC{\equiv}CC_6H_4CH_3\text{-}4)_8(THF)_4]$ has also been determined. A comparison study of the spectroscopic properties of the hexanuclear platinum–silver complex with its precursor complex has been made and their spectroscopic origins were suggested.

Introduction

Over the past decade, the design and construction of discrete, functional supramolecular species has been an intense area of research.[1,2] The square-planar coordination geometry of d^8 metals has attracted a lot of interest and has led to an increasing utilization of d^8 metal complexes as versatile building blocks for self-assembly works.[2] Platinum(II) alkynyl systems have also drawn considerable attention recently in view of their rich optical and redox behavior as well as their reactivity.[3−5] Although tetraalkynylplatinate-

* Corresponding author. E-mail: wwyam@hku.hk. Fax: (852) 2857-1586.

(1) (a) Linton, B.; Hamilton, A. D. *Chem. Rev.* **1997**, *97*, 1669−1680. (b) Slone, R. V.; Yoon, D. I.; Calhoun, R. M.; Hupp, J. T. *J. Am. Chem. Soc.* **1995**, *117*, 11813−11814. (c) Caulder, D. L.; Raymond, K. N. *Acc. Chem. Res.* **1999**, *32*, 975−982. (d) Cotton, F. A.; Dikarev, E. V.; Petrukhina, M. A.; Schmitz, M.; Stang, P. J. *Inorg. Chem.* **2002**, *41*, 2903−2908. (e) Sun, S. S.; Silva, A. S.; Brinn, I. M.; Lees, A. J. *Inorg. Chem.* **2000**, *39*, 1344−1345.

(2) (a) Fujita, M.; Umemoto, K.; Yoshizawa, M.; Fujita, N.; Kusukawa, T.; Biradha, K. *Chem. Commun.* **2001**, 509−518. (b) Leininger, S.; Olenyuk, B.; Stang, P. J. *Chem. Rev.* **2000**, *100*, 853−908. (c) Johannessen, S. C.; Brisbois, R. G. *J. Am. Chem. Soc.* **2001**, *123*, 3818−3819.

(3) (a) ALQaisi, S. M.; Galat, K. J.; Chai, M.; Ray, D. G., III; Rinaldi, P. L.; Tessier, C. A.; Youngs, W. J. *J. Am. Chem. Soc.* **1998**, *120*, 12149−12150. (b) Whiteford, J. A.; Lu, C. V.; Stang, P. J. *J. Am. Chem. Soc.* **1997**, *119*, 2524−2525.

(4) (a) Long, N. J. *Angew. Chem., Int. Ed. Engl.* **1995**, *34*, 21−38. (b) Beck, W.; Niemer, B.; Wieser, M. *Angew. Chem., Int. Ed. Engl.* **1993**, *32*, 923−949. (c) Diederich, F.; Faust, R.; Gramlich, V.; Seiler, P. *J. Chem. Soc., Chem. Commun.* **1994**, 2045−2046. (d) Kaharu, T.; Matsubara, H.; Takahashi, S. *J. Mater. Chem.* **1992**, *2*, 43−47. (e) Hissler, M.; Ziessel, R. *J. Chem. Soc., Dalton Trans.* **1995**, 893−896. (e) Davies, S. J.; Johnson, B. F. G.; Khan, M. S.; Lewis, J. *J. Chem. Soc., Chem. Commum.* **1991**, 187−188.

(5) (a) Yam, V. W. W.; Hui, C. K.; Wong, K. M. C.; Zhu, N.; Cheung, K. K. *Organometallics* **2002**, 21, 4326−4334. (b) Yam, V. W. W.; Tao, C. H.; Zhang, L.; Wong, K. M. C.; Cheung, K. K. *Organometallics* **2001**, *20*, 453−459. (c) Sacksteder, L.; Baralt, E.; DeGraff, B. A.; Lukehart, C. M.; Demas, J. N. *Inorg. Chem.* **1991**, *30*, 2468−2476. (d) Choi, C. L.; Cheng, Y. F.; Yip, C.; Phillips, D. L.; Yam, V. W. W. *Organometallics* **2000**, *19*, 3192−3196. (e) Chan, C. W.; Cheng, L. K.; Che, C. M. *Coord. Chem. Rev.* **1994**, *132*, 87−97. (f) Hissler, M.; Connick, W. B.; Geiger, D. K.; McGarrah, J. E.; Lipa, D.; Lachicotte, R. J.; Eisenberg, R. *Inorg. Chem.* **2000**, *39*, 447−457.

10.1021/ic034877l CCC: $27.50
Published on Web 12/17/2003

(II) complexes $[Pt(C{\equiv}CR)_4]^{2-}$ are known,[6] most of them are confined to the simple monoynyl systems, with corresponding studies on the diynyl system and N-heterocycle-containing alkynyl analogues unexplored. These, together with the numerous studies on the luminescence behavior of platinum(II)−alkynyl systems,[5] and our recent interest in luminescent carbon-rich metal-based molecular materials,[7] in particular our recent work on the assembly of a face-to-face hexanuclear platinum(II)−ethynylpyridine complex,[8] have prompted us to investigate the luminescence properties of $[Pt(C{\equiv}CR)_4]^{2-}$ with N-heterocycle-containing alkynyl ligands, which can potentially be utilized as spectroscopic interesting building blocks. Herein we report the synthesis, luminescence behavior, and structural characterization of a series of platinum(II)−alkynyl complexes of N-heterocycle-containing alkynyls, $(NBu_4)_2[Pt(C{\equiv}CR)_4]$ (R = C_6H_4N-4, C_6H_4N-3, and $C_6H_3N_2$-5). Attempts have also been made to assemble supramolecular entities by employing these complexes as building blocks. Extension of the monoynyl system $[Pt(C{\equiv}CR)_4]^{2-}$ to the diynl system $[Pt(C{\equiv}CC{\equiv}CR)_4]^{2-}$ has also been made. A mixed-metal platinum(II)−silver(I) complex has also been synthesized and studied, through which further insights into the nature of the excited-state origin are provided.

Experimental Section

Materials and Reagents. *n*-Butyllithium (1.6 M in hexane) and $[Ag(MeCN)_4]BF_4$ were purchased from Aldrich Chemical Co. Inc. 4-Bromopyridine hydrogenchloride, 3-pyridine, and 5-bromopyrimidine were purchased from Lancaster Chemical Co. Inc. Trimethylsilylacetylene was purchased from GFS Chemical Co. Ltd. 3-Ethynylpyridine,[9a] 4-ethynylpyridine,[9a] 5-ethynylpyrimidine,[9a] phenylbutadiyne,[9b] tolylbutadiyne,[9b] $[Pt(tht)_2Cl_2]$,[10] and $[Pt(^tBu_3trpy)(MeCN)](OTf)_2$[11] were prepared according to literature procedures. Tetrahydrofuran (THF), toluene, and benzene used for synthesis of the complexes were distilled over sodium benzophenone ketyl and stored under nitrogen atmosphere prior to use. Other solvents such as methanol (Merck, GR), acetonitrile (Lab-Scan, AR), and diethyl ether (Scharlau, AR) were used as received. All other reagents were of analytical grade and were used as received.

Physical Measurements and Instrumentation. ^{1}H NMR spectra were recorded on either a Bruker DPX-300 (300 MHz) or a Bruker Avance 400 (400 MHz) FT-NMR spectrometer. Chemical shifts were recorded relative to tetramethylsilane (Me_4Si). UV−visible spectra were obtained on a Hewlett-Packard 8452A diode array spectrophotometer, IR spectra as Nujol mulls on KBr disks on a Bio-Rad FTS-7 Fourier transform infrared spectrophotometer (4000−400 cm^{-1}), negative FAB mass spectra on a Finnigan MAT95 mass spectrometer, and positive and negative ESI mass spectra on a Finnigan LCQ mass spectrometer. Elemental analyses were performed on a Carlo Erba 1106 elemental analyzer at the Institute of Chemistry in Beijing, Chinese Academy of Sciences. Steady-state emission and excitation spectra at room temperature and at 77 K were obtained on a Spex Fluorolog-2 model F111 fluorescence spectrophotometer with or without Corning filters. The 77 K solid-state emission and excitation spectra were recorded with solid samples loaded in a quartz tube inside a quartz-walled optical Dewar flask filled with liquid nitrogen. For solution emission and excitation spectral studies, the solutions were prepared in a 10 mL Pyrex bulb connected to a sidearm 1-cm quartz cuvette and sealed from the atmosphere by a Rotaflo HP6/6 quick-release Teflon stopper. The solutions were rigorously degassed with no fewer than four freeze−pump−thaw cycles. Emission lifetime measurements were performed with a conventional laser system. The excitation source was the 355 nm output (third harmonic) of a Spectra-Physics Quanta-Ray Q-switched GCR-150-10 pulsed Nd:YAG laser. Luminescence decay signals were recorded on a Tektronix model TDS620A digital oscilloscope and analyzed by use of a program for exponential fits. Luminescence quantum yield was measured by the optical dilute method reported by Demas and Crosby.[12] The luminescence quantum yield of the sample was determined according to

$$\phi_s = \phi_r(B_r/B_s)(n_s/n_r)^2(D_s/D_r) \quad (1)$$

where the subscripts s and r refer to the sample and reference solutions, respectively, $B = 1-10^{-AL}$. A is the absorbance at the excitation wavelength, L is the path length, n is the refractive index of the solvent, and D is the integrated emission intensity. A degassed aqueous solution of quinine sulfate in 1.0 N H_2SO_4 solution (ϕ_{em} = 0.546, excitation wavelength at 365 nm) was used as the reference.[12]

Cyclic voltammetric measurements were performed by using a CH Instruments, Inc. Model CHI 620 electrochemical analyzer, which was interfaced to an IBM-compatible 486 personal computer. The electrolytic cell used was a conventional two-compartment cell. Electrochemical measurements were performed in acetonitrile solutions with 0.1 M $^nBu_4NPF_6$ (TBAH) as supporting electrolyte at room temperature. The reference electrode was a $Ag/AgNO_3$ (0.1 M in acetonitrile) electrode, and the working electrode was a glassy-carbon (Atomergic Chemetal V25) electrode with a piece of platinum wire as counter electrode in a compartment that is separated from the working electrode by a sintered-glass frit. The ferrocenium/ferrocene couple ($FeCp_2^{+/0}$) was used as the internal reference,[13] with the $FeCp_2^{+/0}$ couple being +0.40 V vs SCE. All solutions for electrochemical studies were deaerated with prepurified argon gas just before measurements. Treatment of the electrode surfaces was as reported elsewhere.

Syntheses of Platinum(II) Alkynyl Complexes. All reactions were carried out under strictly anaerobic and anhydrous conditions in an inert atmosphere of nitrogen by standard Schlenk technique. Synthetic routes to complexes **1**−**7** are summarized in Scheme 1.

(6) Espinet, P.; Fornies, J.; Martinez, F.; Tomas, M. *J. Chem. Soc., Dalton Trans.* **1990**, 791−798.
(7) (a) Yam, V. W. W. *Acc. Chem. Res.* **2002,** *35*, 555−563. (b) Yam, V. W. W. *Chem. Commun.* **2001**, 789−796. (c) Yam, V. W. W.; Lo, W. Y.; Lam, C. H.; Fung, W. K. M.; Wong, K. M. C.; Lau V. C. Y.; Zhu, N. *Coord. Chem. Rev.* **2003**, in press. (d) Wong, K. M. C.; Hui, C. K.; Yu, K. L.; Yam, V. W. W. Yam *Coord. Chem. Rev.* **2002**, *229*, 123−132. (e) Yam, V. W. W.; Wong, K. W. M. C.; Zhu, N. *J. Am. Chem. Soc.* **2002**, *124*, 6506−6507. (f) Yam, V. W. W.; Wong, K. M. C.; Zhu, N. *Angew. Chem., Int. Ed.* **2003**, *42*, 1400−1403. (g) Tao, C. H.; Wong, K. W. M. C.; Zhu, N.; Yam, V. W. W. *New J. Chem.* **2003**, *27*, 150−154.
(8) Hui, C. K.; Chu, B. W. K.; Zhu, N.; Yam, V. W. W. *Inorg. Chem.* **2002**, *41*, 6178−6180.
(9) (a) Kim, W. H.; Kodali, N. B.; Kumar, J.; Tripathy, S. K. *Macromolecules* **1994**, *27*, 1819−1824. (b) Eastmond, R.; Walton, D. R. M. *Synthesis* **1983**, 128−130.
(10) Uson, R.; Fornies, J.; Martinez, F.; Tomas, M. *J. Chem. Soc., Dalton Trans.* **1980**, 888−894.
(11) Yam, V. W. W.; Tang, R. P. L.; Wong, K. M. C.; Cheung, K. K. *Organometallics* **2001**, *20*, 4476−4482.
(12) Demas, J. N.; Crosby, G. A. *J. Phys. Chem.*, **1971**, *75*, 991−1023.
(13) (a) Connelly, N. G and Geiger, W. E. *Chem. Rev.* **1996**, *96*, 877−910. (b) Gagne, R. R.; Koval, C. A.; Lisensky, G. C. *Inorg. Chem.* **1980**, *19*, 2854−2855.

Scheme 1. Synthetic Routes to Complexes **1**−**7**

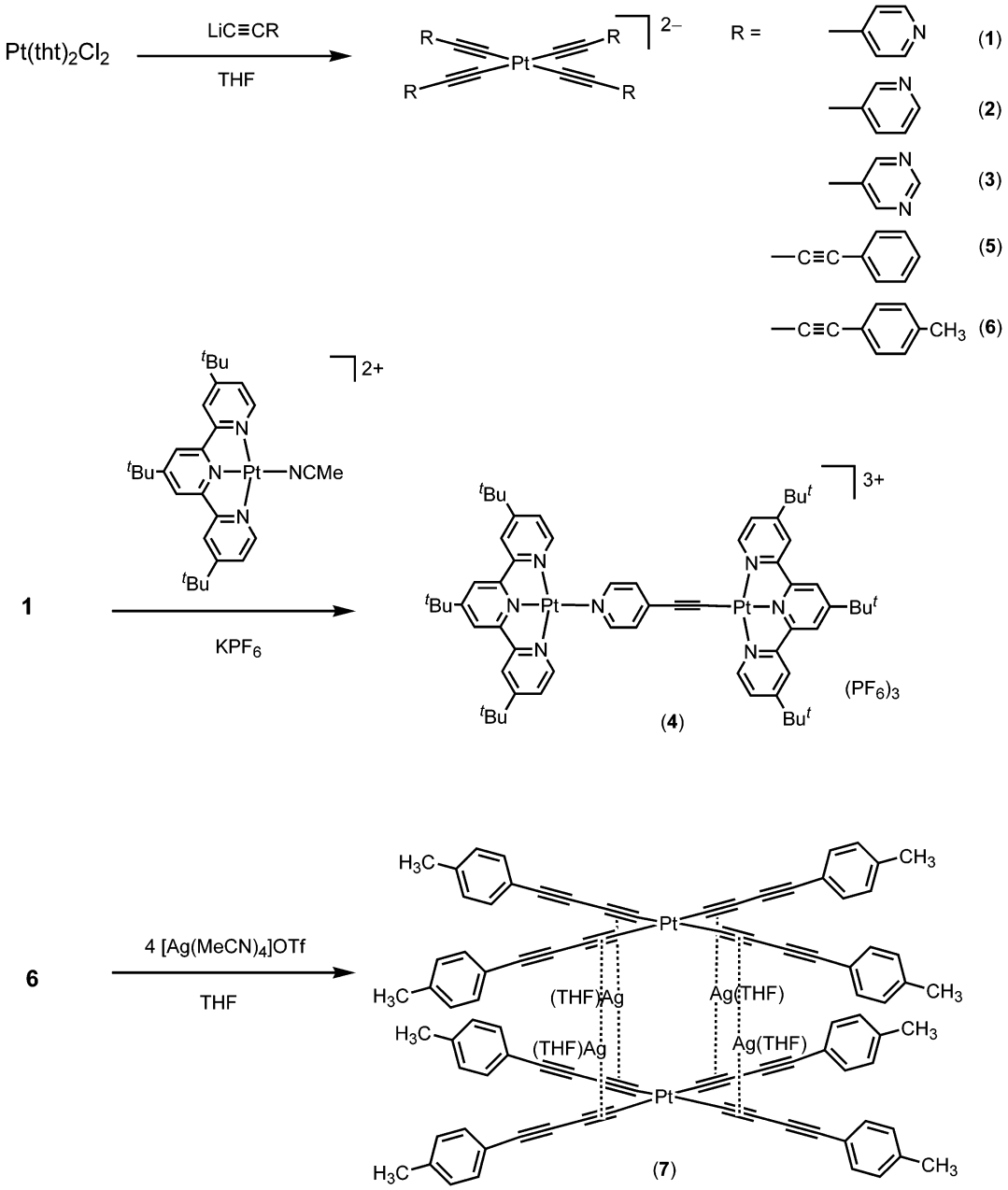

$(Bu_4N)_2[Pt(C{\equiv}CC_5H_4N\text{-}4)_4]$ (1). The complex was prepared by a slight modification of the method reported for the preparation of $[^nBu_4N]_2[Pt(C{\equiv}CPh)_4]$.[6] *n*-Butyllithium (1.6 M in *n*-hexane, 0.63 mL, 1.0 mmol) was added to a solution of $HC{\equiv}CC_5H_4N$-4 (110 mg, 1.1 mmol) in dry THF (20 mL) at −78 °C and stirred for 30 min. The cooling bath was then removed and the mixture was slowly warmed to room temperature. $[Pt(tht)_2Cl_2]$ (tht = tetrahydrothiophene) (105 mg, 0.18 mmol) was added and the reaction mixture was stirred at room temperature for an additional 24 h. The resulting solution was evaporated to dryness and the residue was dissolved in a minimum amount of deoxygenated deionized water. The resulting pale yellow solution was added dropwise to a solution of $^nBu_4NCl$ (100 mg, 0.36 mmol) in isopropyl alcohol (0.5 mL) to give **1** as a yellow precipitate. Subsequent recrystallization from dichloromethane−diethyl ether yielded **1** as yellow crystals. Yield: 120 mg, 62%. ^1H NMR (300 MHz, $CDCl_3$, 298 K, relative to $SiMe_4$): δ 0.89 (t, 24H, $[CH_3(CH_2)_2CH_2)_4N^+$, J = 8.1 Hz], 1.50−1.67 [m, 32H, $(CH_3(CH_2)_2CH_2)_4N^+$], 3.57 [m, 16H, $(CH_3(CH_2)_2CH_2)_4N^+$], 7.10 (d, 8H, pyridyl H meta to N, J = 5.9 Hz), 8.33 (8H, pyridyl H ortho to N, J = 5.9 Hz). Negative ESI-MS: ion clusters at *m*/*z* 846 $[M - {}^nBu_4N^+]^-$. Anal. Calcd for $C_{60}H_{88}N_6Pt$: C, 66.21; H, 8.15; N, 7.72%. Found: C, 66.42; H, 8.17; N, 7.75%.

$(Bu_4N)_2[Pt(C{\equiv}CC_5H_4N\text{-}3)_4]$ (2). The procedure was similar to that described for the preparation of **1** except $HC{\equiv}CC_5H_4N$-3 (110 mg, 1.1 mmol) was used in place of $HC{\equiv}CC_5H_4N$-4. Yield: 117 mg, 60%. ^1H NMR (300 MHz, $CDCl_3$, 298 K, relative to $SiMe_4$): δ 0.89 [t, 24H, $(CH_3(CH_2)_2CH_2)_4N^+$, J = 7.9 Hz], 1.52−1.64 [m, 32H, $(CH_3(CH_2)_2CH_2)_4N^+$], 3.52 [m, 16H, $(CH_3(CH_2)_2CH_2)_4N^+$], 7.15 (m, 4H, pyridyl H at 5-position), 7.61 (m, 4H, pyridyl H at 4-position), 8.25 (m, 4H, pyridyl H at 6-position), 8.56 (s, 4H, pyridyl H at 2-position). Negative ESI-MS: ion clusters at *m*/*z* 846 $[M - {}^nBu_4N^+]^-$. Anal. Calcd for $C_{60}H_{88}N_6Pt$: 66.21; H, 8.15; N, 7.72%. Found: 65.69; H, 7.96; N, 7.69%.

$(Bu_4N)_2[Pt(C{\equiv}CC_4H_3N_2\text{-}5)_4]$ (3). The procedure was similar to that described for the preparation of **1** except $HC{\equiv}CC_4H_3N_2$-5 (114 mg, 1.1 mmol) was used in place of $HC{\equiv}CC_5H_4N$-4. Yield: 128

mg, 65%. ^{1}H NMR (400 MHz, $CDCl_3$, 298 K, relative to $SiMe_4$): δ 0.86 [t, 24H, ($CH_3(CH_2)_2CH_2)_4N^+$, J = 7.3 Hz], 1.43 [m, 16H, ($CH_3CH_2(CH_2)_2)_4N^+$], 1.61 [m, 16H, ($CH_3CH_2CH_2CH_2)_4N^+$], 3.61 [m, 16H, $CH_3(CH_2)_2CH_2N^+$], 8.58 (s, 8H, pyrimidyl H at 4- and 6-position), 8.87 (s, 4H, pyrimidyl H at 2-position). Negative ESI-MS: ion clusters at m/z 850 [M − ^{n}Bu$_4$N$^+$]$^-$. Anal. Calcd for $C_{56}H_{84}N_{10}Pt$: C, 61.57; H, 7.75; N, 12.82%. Found: C, 61.52; H, 7.88; N, 12.87%.

[Pt(^{t}Bu$_3$trpy)(C≡CC$_5$H$_4$N-4)Pt(^{t}Bu$_3$trpy)](PF$_6$)$_3$ (4). $(Bu_4N)_2$[Pt(C≡CC$_5$H$_4$N-4)$_4$] (**1**) (0.05 g, 0.05 mmol) was suspended in dry methanol (10 mL), 4 equiv of [Pt(^{t}Bu$_3$trpy)(MeCN)](OTf)$_2$ (0.10 g, 0.10 mmol) dissolved in methanol (5 mL) was added, and the mixture was stirred for 3 h to give a clear bright orange solution. NH_4PF_6 dissolved in methanol was added dropwise to give an orange-yellow crystalline solid. Subsequent recrystallization from dichloromethane−diethyl ether afforded **4** as air-stable orange-yellow crystals. Yield: 63 mg, 75%. ^{1}H NMR (300 MHz, $CDCl_3$, 298 K, relative to $SiMe_4$): δ 1.66 [m, 54H, (CH_3)$_3$C-], 8.05 [dd, 2H, 5,5″-terpyridyl H's on (^{t}Bu$_3$trpy)Pt−C≡C, J = 6.1, 2.1 Hz], 8.14 [m, 4H, 6,6″-terpyridyl H's on (^{t}Bu$_3$trpy)Pt−C≡C and 5,5″-terpyridyl H's on (^{t}Bu$_3$trpy)Pt−N], 8.25 (d, 2H, pyridyl H's ortho to C≡C, J = 6.1 Hz), 8.90 [d, 2H, 3,3″-terpyridyl H's on (^{t}Bu$_3$trpy)Pt−C≡C, J = 2.1 Hz], 8.99 [m, 6H, 3′,5′-terpyridyl H's on (^{t}Bu$_3$trpy)Pt−C≡C and 3,3′,5′,3″-terpyridyl H's on (^{t}Bu$_3$trpy)Pt−N], 9.12 [d, 2H, 6,6″- terpyridyl H's on (^{t}Bu$_3$trpy)Pt−C≡C, J = 5.4 Hz], 9.39 (d, 2H, pyridyl H meta to C≡C, J = 6.1 Hz). Positive ESI-MS: ion clusters at m/z 1584 [M − PF_6^-]$^+$. Anal. Calcd for $C_{61}H_{74}N_7P_3F_{18}Pt_2$: C, 42.34; H, 4.31; N, 5.67%. Found: C, 42.48; H, 4.28; N, 5.21%.

(Bu$_4$N)$_2$[Pt(C≡CC≡CC$_6$H$_5$)$_4$] (5). The procedure was similar to that described for the preparation of **1** except HC≡CC≡CC$_6$H$_5$ (140 mg, 1.1 mmol) was used in place of HC≡CC$_5$H$_4$N-4. Yield: 159 mg, 75%. ^{1}H NMR (300 MHz, $CDCl_3$, 298 K, relative to $SiMe_4$): δ 0.89 [t, 24H, ($CH_3(CH_2)_2CH_2)_4N^+$, J = 8.1 Hz], 1.50−1.63 [m, 32H, ($CH_3(CH_2)_2CH_2)_4N^+$], 3.57 [m, 16H, ($CH_3(CH_2)_2CH_2)_4N^+$], 7.25 (m, 12H, aryl H para and meta to C≡C), 7.38 (m, 8H, aryl H ortho to C≡C). Negative FAB-MS: ion clusters at m/z 938 [M − ^{n}Bu$_4$N$^+$]$^-$. Anal. Calcd for $C_{72}H_{92}N_2Pt$: C, 73.25; H, 7.85; N, 2.37%. Found: C, 73.55; H, 7.62; N, 2.25%.

(Bu$_4$N)$_2$[Pt(C≡CC≡CC$_6$H$_4$CH$_3$-4)$_4$] (6). The procedure was similar to that described for the preparation of **1** except HC≡CC≡CC$_6$H$_4$CH$_3$-4 (155 mg, 1.1 mmol) was used in place of HC≡CC$_5$H$_4$N-4. Yield: 156 mg, 70%. ^{1}H NMR (300 MHz, $CDCl_3$, 298 K, relative to $SiMe_4$): δ 1.02 [t, 24H, ($CH_3(CH_2)_2CH_2)_4N^+$, J = 8.1 Hz], 1.50−1.63 [m, 32H, ($CH_3(CH_2)_2CH_2)_4N^+$], 2.75 (s, 12H, CH_3), 3.52 [m, 16H, ($CH_3(CH_2)_2CH_2)_4N^+$], 7.12 (d, 8H, aryl H meta to C≡C, J = 8.0 Hz), 7.29 (d, 8H, aryl H ortho to C≡C, J = 8.0 Hz). Negative FAB-MS: ion clusters at m/z 994 [M − ^{n}Bu$_4$N$^+$]$^-$. Anal. Calcd for $C_{76}H_{100}N_2Pt$: C, 73.81; H, 8.15; N, 2.27%. Found: C, 73.60; H, 8.02; N, 2.12%.

[Pt$_2$Ag$_4$(C≡CC≡CC$_6$H$_4$CH$_3$-4)$_8$(THF)$_4$] (7). The complex was prepared by modification of a literature-reported method.[6] A solution of [Ag(MeCN)$_4$][BF_4] (0.03 g, 0.084 mmol) in THF (10 mL) was added dropwise to a solution of [^{n}Bu$_4$N]$_2$[Pt(C≡CC≡CC$_6$H$_4$CH$_3$-4)$_4$] (**6**) (0.05 g, 0.041 mmol) in THF (10 mL). The mixture was allowed to stir at room temperature for 3 h. The reaction mixture was then filtered and a clear orange-red solution was obtained. The solution was reduced in volume and subsequent recrystallization by layering diethyl ether yielded **7** as air-stable garnet crystals. Yield: 0.035 mg, 88%. ^{1}H NMR (300 MHz, $CDCl_3$, 298 K, relative to $SiMe_4$): δ 7.24 (m, 12H, aryl H meta and para to C≡C), 7.39 (m, 8H, aryl H ortho to C≡C). IR (Nujol mull, KBr), ν/cm^{-1} (C≡C) 2047m. Negative ESI-MS: ion clusters at m/z 1827 [M − Ag$^+$]$^-$. Anal. Calcd for $C_{88}H_{56}Ag_4Pt_2$·0.5THF: C, 54.62; H, 2.92%. Found: C, 54.84; H, 3.06%.

Crystal Structure Determination. Crystal data for **4**, $C_{71}H_{94}Cl_{10}F_{18}N_7P_3Pt_2$, formula weight = 2225.12, triclinic, space group $P\bar{1}$, a = 13.514(3) Å, b = 20.006(4) Å, c = 20.297(4) Å, α = 62.07(3)°, β = 81.59(3)°, γ = 76.24(3)°, V = 4705.3(16) Å^3, Z = 2, D_c = 1.571 g cm^{-3}, μ(Mo Kα) = 33.81 cm^{-1}, F(000) = 2204, T = 293 K, are summarized in Table 1. A crystal of dimensions 0.40 × 0.15 × 0.04 mm inside a glass capillary was used for data collection at 20 °C on a MAR diffractometer with a 300 mm image plate detector by use of graphite-monochromated Mo Kα radiation (λ = 0.71073 Å). Data collection was made with 2° oscillation (90 images) at 120 mm distance and 480 s exposure. The images were interpreted and intensities integrated by use of the program *DENZO*.[14] From a total of 18 308 measured reflections, 11 984 unique reflections were obtained (R_{int} = 0.0400), and 7097 reflections with $I > 4\sigma(I)$ were considered and used in the structural analysis. These reflections were in the range h = −14 to 15, k = −23 to 23, and l = −22 to 22 with $2\theta_{max}$ = 50.70°. The structure was solved by direct methods employing the SIR-97 program[15] on PC. Pt and many non-hydrogen atoms were located according to direct methods and the successive least-squares Fourier cycles. The positions of other non-hydrogen atoms were found by successful full-matrix least-squares refinements and successive difference Fourier synthesis by use of the program SHELXL-97[16] on PC. Three anions of PF_6^- were located. In the asymmetric unit, five 1,2-dichloroethane solvent molecules were located in seven positions. One of the solvent molecules is disordered into two sets of positions, sharing one Cl atom. Half of the solvent molecule has too-high thermal parameters and was considered to be partially located, thus atoms of the solvent molecules were set to have 0.5 occupancy. For convergence of least-squares refinements, restraints had to be applied for the solvent molecules to be near 1.50(2) Å. Meanwhile, thermal parameters of C(70) and C(71) were assumed to be the same. One crystallographic asymmetric unit consists of one formula unit, including three anions and five solvent molecules. In the final stage of least-squares refinement, atoms of solvent molecules [except Cl(1)−Cl(4)] were refined isotropically and other non-hydrogen atoms were refined isotropically. H atoms were generated by the program SHELXL-97. The positions of H atoms were calculated on the basis of riding mode, with thermal parameters equal to 1.2 times those of the associated C atoms, and participated in the calculation of final R-indices. Convergence for 939 variable parameters by least-squares refinement on F with $w = 4F_o^2/\sigma^2(F_o^2)$, where $\sigma^2(F_o^2) = [\sigma^2(I) + (0.029F_o^2)^2]$ for 5191 reflections with $I > 4\sigma(I)$, was reached at R = 0.0591 and wR = 0.1603 with a goodness-of-fit of 0.932. $(\Delta/\sigma)_{max}$ = 0.001. The final difference Fourier map shows maximum rest peaks and holes of 1.058 and −1.277 e Å^{-3}, respectively.

Crystal data for **7**, $C_{112}H_{108}Ag_4O_6Pt_2$, formula weight = 2371.64, monoclinic, space group $C2/c$, a = 26.059(5) Å, b = 15.965(3) Å, c = 25.021(5) Å, α = 90°, β = 91.17(3)°, γ = 90°, V = 10.407(3) Å^3, Z = 4, D_c = 1.514 g cm^{-3}, μ(Mo Kα) = 34.66 cm^{-1}, F(000) = 4688, T = 253 K, are summarized in Table 1. A crystal of

(14) *DENZO*: *The HKL Manual*—A description of programs *DENZO*, *XDISPLAYF*, and *SCALEPACK*, written by D. Gewirth with the cooperation of the program authors Z. Otwinowski and W. Minor, 1995, Yale University, New Haven, CT.

(15) *SIR97*: Altomare, A.; Burla, M. C.; Camalli, M.; Cascarano, G. L.; Giacovazzo, C.; Guagliardi, A.; Moliterni, A. G. G.; Polidori, G.; Spagna, R. *J. Appl. Crystallogr.* **1999**, *32*, 115−119.

(16) *SHELXL97*: Sheldrick, G. M. *SHELX97*: Programs for Crystal Structure Analysis (Release 97-2), 1997, University of Goettingen, Germany.

Table 1. Crystal and Structure Determination Data of [Pt(^{t}Bu$_3$trpy)(C≡CC$_5$H$_4$N)Pt(^{t}Bu$_3$trpy)](PF$_6$)$_3$ (**4**) and [Pt$_2$Ag$_4$(C≡CC≡CC$_6$H$_4$CH$_3$-4)$_8$(THF)$_4$] (**7**)

	4	**7**
formula	$C_{71}H_{94}Cl_{10}F_{18}N_7P_3Pt_2$	$C_{112}H_{108}Ag_4O_6Pt_2$
fw	2225.12	2371.64
T, °C	293	253
a, Å	13.514(3)	26.059(5)
b, Å	20.006(4)	15.965(3)
c, Å	20.297(4)	25.021(5)
α, deg	60.07(3)	90
β, deg	81.59(3)	91.17(3)
γ, deg	76.24(3)	90
V, Å^3	4705.3(16)	10,407(3)
cryst syst	triclinic	monoclinic
space group	$P\bar{1}$	$C2/c$
Z	2	4
F(000)	2204	4688
D_c, g cm^{-3}	1.571	1.514
cryst color	yellow	yellow
cryst dimens, mm	0.20 × 0.15 × 0.06	0.40 × 0.25 × 0.15
λ, Å (graphite monochromated, Mo Kα)	0.710 73	0.710 73
μ, cm^{-1}	33.81	34.66
collection range, deg	$2\theta_{max} = 50.07$	$2\theta_{max} = 50.3$
h	−14 to 15	−27 to 27
k	−23 to 23	−18 to 18
l	−22 to 22	−28 to 27
no. of data collected	18 308	13 953
no. of unique data	11 984	6005
no. of data used in refinement, m	7097	3034
no. of params refined, p	939	485
R	0.0591	0.0570
R_w[a]	0.1603	0.1447
S	0.932	0.982
max. shift, (shift/error)$_{max}$	0.01	0.001
residual extrema in final diff map, e Å^{-3}	+1.058, −1.277	+0.968, −2.200

[a] $w = 1/[\sigma^2(F_o^2) + (aP)^2 + bP]$, where $P = [2F_c^2 + \max(F_o^2,0)]/3$.

dimensions 0.40 × 0.25 × 0.15 mm inside a glass capillary was used for data collection at −20 °C on a MAR diffractometer with a 300 mm image plate detector by use of graphite-monochromated Mo Kα radiation ($\lambda = 0.710\ 73$ Å). Data collection was made with 1.5° oscillation (140 images) at 120 mm distance and 420 s exposure. The images were interpreted and intensities integrated by use of the program *DENZO*.[14] From a total of 13 953 measured reflections, 11 984 unique reflections were obtained ($R_{int} = 0.0543$), and 3034 reflections with $I > 4\sigma(I)$ were considered and used in the structural analysis. These reflections were in the range $h = -27$ to 27, $k = -18$ to 18, and $l = -28$ to 27 with $2\theta_{max} = 50.30°$. The structure was solved by direct methods employing the SIR-97 program[15] on PC. One crystallographic asymmetric unit consists of half of a formula unit, including one diethyl ether solvent molecule. In final stage of least-squares refinement, non-H atoms of diethyl ether were refined isotropically, and other non-H atoms were refined anisotropically. The H atoms were generated by SHELXL-97[16] on PC. The positions of H atoms were calculated on the basis of riding mode, with thermal parameters equal to 1.2 times those of the associated C atoms, and participated in the calculation of final R-indices. Convergence for 485 variable parameters by least-squares refinement on F with $w = 4F_o^2/\sigma^2(F_o^2)$, where $\sigma^2(F_o^2) = [\sigma^2(I) + (0.029F_o^2)^2]$ for 3034 reflections with $I > 4\sigma(I)$, was reached at $R = 0.0570$ and $wR = 0.1447$ with a goodness-of-fit of 0.877. $(\Delta/\sigma)_{max} = 0.001$. The final difference Fourier map shows maximum rest peaks and holes of 0.968 and −2.200 e Å^{-3}, respectively.

Results and Discussion

Complexes **1**−**3** were synthesized according to a literature procedure for (^{n}Bu$_4$N)$_2$[Pt(C≡CPh)$_4$][6] with modifications. Treatment of [Pt(tht)$_2$Cl$_2$] with the corresponding LiC≡CR in THF, followed by a metathesis reaction with ^{n}Bu$_4$NCl in deoxygenated water, and subsequent recrystallization by diffusion of diethyl ether vapor into a concentrated dichloromethane solution of the respective complexes afforded the products as pale yellow crystals in good yield. Under similar conditions, their diynyl analogues **5** and **6** were also successfully synthesized and characterized. Reaction of **1** with 4 equiv of [Pt(^{t}Bu$_3$trpy)(MeCN)](OTf)$_2$ in methanol did not yield the desired pentanuclear platinum product, [Pt(C≡CC$_5$H$_4$N)$_4${Pt(^{t}Bu$_3$trpy)}$_4$](OTf)$_6$, but instead crystals of [Pt(^{t}Bu$_3$trpy)(C≡CC$_5$H$_4$N)Pt(^{t}Bu$_3$trpy)](PF$_6$)$_3$ (**4**) were obtained after the metathesis reaction with ammonium hexafluorophosphate. The formation of compound **4** via alkynyl group transfer is less commonly observed in other platinum alkynyl systems[17] and may probably be a result of the relative instability of the tetraalkynylplatinate(II) system, which renders the transmetalation reaction more likely to occur. Reaction of complex **6** with [Ag(MeCN)$_4$][BF$_4$] according to a modified literature procedure[18a] yielded air-stable complexes of [Pt$_2$Ag$_4$(C≡CC≡CC$_6$H$_4$CH$_3$-4)$_8$(THF)$_4$] (**7**). Subsequent recrystallization from layering of *n*-hexane onto a THF solution of **7** afforded **7** as orange crystals in almost quantitative yield. The identities of the complexes have been established by ^{1}H and ^{31}P NMR, fast atom bombardment

(17) (a) Hui, C. K.; Chu, B. W. K.; Zhu, N.; Yam, V. W. W. *Inorg. Chem.* **2002**, *41*, 6178. (b) Whiteford, J. A.; Lu, C. V.; Stang, P. J. *J. Am. Chem. Soc.* **1997**, *119*, 2524.

(18) (a) Yam, V. W. W.; Yu, K. L.; Cheung, K. K. *J. Chem. Soc., Dalton Trans.* **1999**, 2913−2915. (b) Charmant, J. P. H.; Fornies, J.; Gornez, J.; Lalinde, E.; Merino, R. I.; Moreno, M. T.; Orpen, A. G. *Organometallics* **1999**, *18*, 3353−3358.

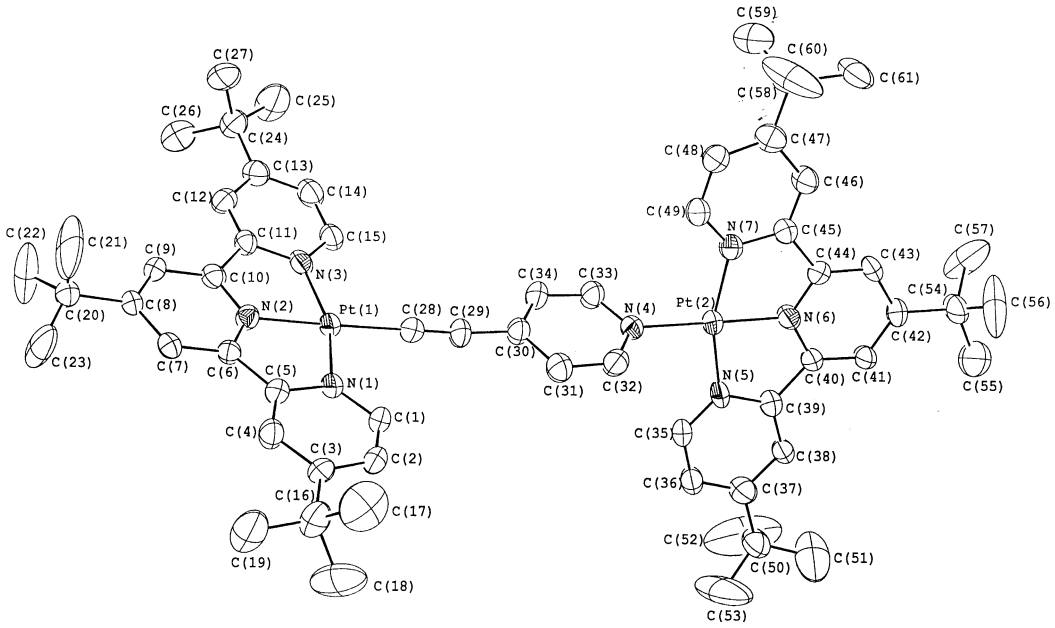

Figure 1. Perspective drawing of the complex cation of **4** with atomic numbering scheme. The H atoms have been omitted for clarity. Thermal ellipsoids are shown at 30% probability level.

Table 2. Selected Bond Distances and Angles for [Pt(^{t}Bu$_3$trpy)(C≡CC$_5$H$_4$N)Pt(^{t}Bu$_3$trpy)](PF$_6$)$_3$ (**4**) and [Pt$_2$Ag$_4$(C≡CC≡CC$_6$H$_4$CH$_3$-4)$_8$(THF)$_4$] (**7**)

[Pt(^{t}Bu$_3$trpy)(C≡CC$_5$H$_4$N)Pt(^{t}Bu$_3$trpy)](PF$_6$)$_3$ (**4**)			
Bond Distances (Å)			
Pt(1)−N(1)	2.03(1)	Pt(2)−N(4)	2.04(1)
Pt(1)−N(2)	1.97(1)	Pt(2)−N(5)	1.99(1)
Pt(1)−N(3)	2.03(1)	Pt(2)−N(6)	1.94(1)
Pt(1)−C(28)	1.98(1)	Pt(2)−N(7)	2.01(1)
C(28)−C(29)	1.20(2)	C(29)−C(30)	1.41(2)
Bond Angles (deg)			
N(1)−Pt(1)−N(2)	80.3(4)	N(5)−Pt(2)−N(6)	80.9(4)
N(2)−Pt(1)−N(3)	80.7(4)	N(6)−Pt(2)−N(7)	80.7(4)
N(1)−Pt(1)−N(3)	161.0(4)	N(5)−Pt(2)−N(7)	161.5(4)
Pt(1)−C(28)−C(29)	178.9(12)	N(2)−Pt(1)−C(28)	176.9(4)
[Pt$_2$Ag$_4$(C≡CC≡CC$_6$H$_4$CH$_3$-4)$_8$(THF)$_4$] (**7**)			
Bond Distances (Å)			
Pt(1)−C(1)	2.08(2)	C(14)−C(15)	1.16(2)
Pt(1)−C(12)	2.01(2)	Pt(1)− Pt (2)	4.47(1)
Pt(2)−C(23)	2.02(2)	Ag(1)−C(1)	2.29(1)
Pt(2)−C(34)	1.97(2)	Ag(1)−C(2)	2.53(2)
C(12)−C(13)	1.21(2)	Ag(1)−C(23)	2.32(2)
C(13)−C(14)	1.40(2)	Ag(1)−C(34)	2.53(2)
Bond Angles (deg)			
C(12)−Pt(1)−C(12)*	177.0(7)	C(23)−Pt(2)−C(23)*	176.9(8)
C(1)−Pt(1)−C(12)	92.1(6)	C(23)−Pt(2)−C(34)	92.3(8)
Pt(1)−C(1)−C(2)	179.1(17)	Pt(2)−C(23)−C(24)	177.1(15)
C(1)−C(2)−C(3)	175.4(18)	C(23)−C(24)−C(25)	175.0(20)
Pt(1)−C(1)−Ag(1)	91.3(6)	Pt(2)−C(23)−Ag(1)	93.6(6)
C(2)−C(1)−Ag(1)	88.3(12)	C(24)−C(23)−Ag(1)	86.2(12)

[a] With estimated standard deviations in parentheses.

(FAB) and electrospray ionization (ESI) mass spectrometry (MS), and elemental analyses. Complexes **4** and **7** have also been characterized crystallographically.

Figure 1 shows the perspective drawing of the complex cation of **4**, and selected bond distances and angles are given in Table 2. The coordination geometry about the platinum centers is essentially distorted square planar, with the bond distance of the platinum to the central nitrogen atom [Pt(1)−N(2), 1.97 Å; Pt(2)−N(6), 1.94 Å] of the terpyridine ligand slightly shorter than that to the other two outer nitrogen atoms [Pt(1)−N(1), 2.03 Å, and Pt(1)−N(3), 2.03 Å; Pt(2)−N(5), 1.99 Å, and Pt(2)−N(7), 2.01 Å], as is required by the steric demand of the terpyridine ligand. All the Pt−N distances are in the range generally observed in typical platinum terpyridine complexes.[7e−g,19] Not surprisingly, the N−Pt−N angles [N(1)−Pt(1)−N(2), 80.3°, N(2)−Pt(1)−N(3), 80.7°, and N(1)−Pt(1)−N(3), 161.0°; N(5)−Pt(2)−N(6), 80.9°, N(6)−Pt(2)−N(7), 80.7°, and N(5)−

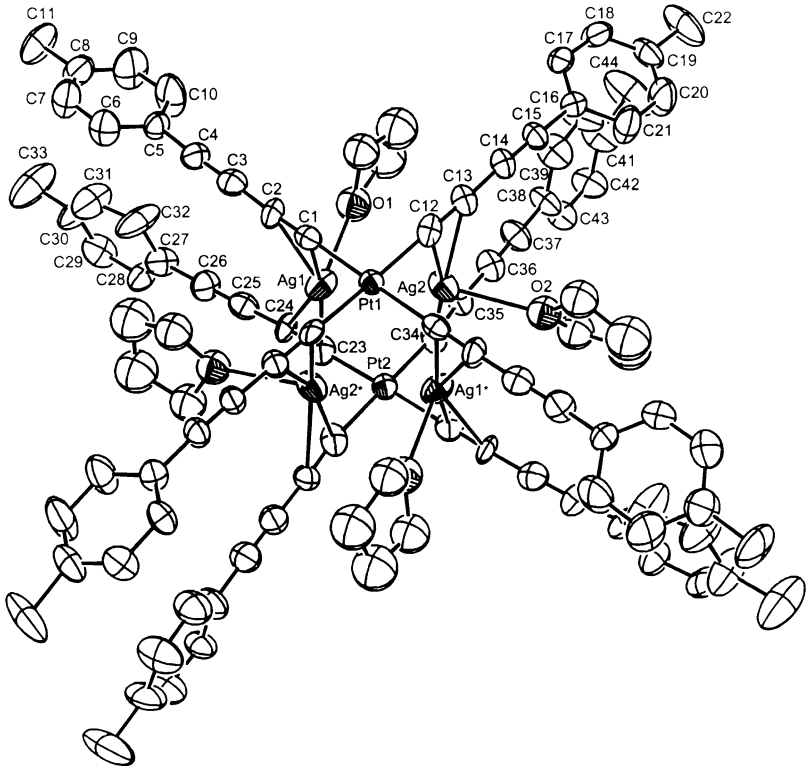

Figure 2. Perspective drawing of **7** with atomic numbering scheme. The H atoms have been omitted for clarity. Thermal ellipsoids are shown at 30% probability level.

Pt(2)−N(7), 161.5°] deviate from the idealized values of 90° and 180° as a consequence of the geometric constraints imposed by the terpyridine ligands. The Pt−C bond distance of 1.98(1) Å and the C≡C bond length of 1.20(2) Å are comparable to those found in other related platinum(II)−alkynyl complexes.[18,20] The Pt−C≡C− unit is essentially linear with a bond angle of 178.9(2)°, while the pyridine ring of the alkynyl ligand is almost parallel to the plane of C≡C-connected platinum−terpyridine with a dihedral angle of 0.83°. On the contrary, the plane of the pyridine ring is almost orthogonal to that of the N-connected platinum−terpyridine with a dihedral angle of 64.12°. This near-orthogonal orientation has also been observed in Pt(C∧N∧C)[21] and Pt(C∧N∧N)[19,22] moieties with ancillary pyridine ligands.

Figure 2 shows the perspective drawing of complex **7**, and selected bond distances and angles are given in Table 2. The structure of **7** shows a distorted octahedral array of Pt_2Ag_4 consisting of two platinum metal centers in a mutually trans disposition and the four silver atoms in the equatorial plane, which are bonded by the inner C≡C units of the platinum diynyl moieties in a π-coordination mode and are coordinated to one THF molecule each. The two square-planar [Pt(C≡CC≡C$C_6H_4CH_3$-4)$_4$] fragments are found to be almost eclipsed, with a torsional angle Pt(1)−C(1)−Pt(2)−C(9) of 7.8° between adjacent fragments. The silver−alkynyl π bonds are asymmetric, with the Ag−C(alkynyl) distances being in the range of 2.28(2)−2.53(2) Å. The C≡C distances are in the range of 1.17(2)−1.22(2) Å, similar to those found in uncoordinated alkynes and σ,π-alkynyl complexes.[18] The Pt−C≡C−C chains are found to be nearly linear, having angles in the range of 177.1(15)−179.1(17)°. The Pt−C(α) distances are found to be almost identical [1.97(2)−2.08(2) Å] and the C−Pt−C angles between two *cis*-alkynyl groups are close to 90° [92.1(6)−92.3(8)°].

The electronic absorption spectra of complexes **1**−**3** in dichloromethane show two intense absorption bands at 290−305 nm and 342−348 nm (see representative spectrum in Figure 3). Similar absorption patterns are observed in complexes **5** and **6** except that the high-energy bands at 276−360 nm are vibronic-structured with vibrational progressional spacings of ca. 1300 cm^{-1}, typical of the ν(C⋯C) stretch of the aromatic moiety, and the low-energy absorption band is shifted to the red at ca. 388−390 nm. Table 3 summarizes the photophysical data of the platinum(II)−alkynyl complexes. The absorption energies of both bands in **1**−**3**, **5**, and **6** are found to depend on the nature of the alkynyl

(19) (a) Aldridge, T. K.; Stacy, E. M.; McMillin, D. R. *Inorg. Chem.* **1994**, *33*, 722. (b) Lai, S. W.; Chan, M. C. W.; Cheung, K. K.; Che, C. M. *Inorg. Chem.* **1999**, *38*, 4262−4267. (c) Tzeng, B. C.; Fu, W. F.; Che, C. M.; Chao, H. Y.; Cheung, K. K.; Peng, S. M. *J. Chem. Soc., Dalton Trans.* **1999**, 1017.

(20) (a) Stahl, J.; Bohling, J. C.; Bauer, E. B.; Peters, T. B.; Mohr, W.; Alvarez, J. M. M.; Hampel, F.; Gladysz, J. A. *Angew. Chem., Int. Ed.* **2002**, *41*, 1871−1876. (b) Mohr, W.; Stahl, J.; Hampel, F.; Gladysz, J. A. *Chem. Eur. J.* **2003**, *9*, 3324−3340. (c) Onitsuka, K.; Fujimoto, M.; Ohshiro, N.; Takahashi, S. *Angew. Chem., Int. Ed.* **1999**, *38*, 689−690. (d) Leininger, S.; Stang, P. J. *Organometallics* **1998**, *17*, 3981−3983. (e) Osakada, K.; Hamada, M.; Yamamoto, T. *Organometallics* **2000**, *19*, 458−468. (f) Falvello, L. R.; Fornies, J.; Gomez, J.; Lalinde, E.; Martin, A.; Martinez, F.; Moreno, M. T. *J. Chem. Soc., Dalton. Trans.* **2001**, 2132−2140. (g) Ara, I.; Berenguer, J. R.; Eguizabal, E.; Fornies, J.; Gomez, J.; Lalinde, E.; Saez-Rocher, J. M. *Organometallics* **2000**, *19*, 4385−4297.

(21) (a) Cave, G. W. V.; Alcock, N. W.; Rourke, J. P. *Organometallics* **1999**, *18*, 1801−1803. (b) Cave, G. W. V.; Fanizzi, F. P.; Deeth, R. J.; Errington, W.; Rourke, J. P. *Organometallics* **2000**, *19*, 1355−1364.

(22) Wong, K. H.; Cheung, K. K.; Chan, M. C. W.; Che, C. M. *Organometallics* **1998**, *17*, 3505−3511.

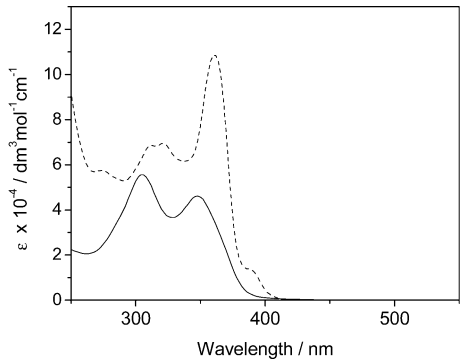

Figure 3. Electronic absorption spectra of $(Bu_4N)_2[Pt(C{\equiv}CC_5H_4N\text{-}4)_4]$ (**1**) (—) and $(Bu_4N)_2[Pt(C{\equiv}CC{\equiv}CC_6H_5)_4]$ (**5**) (- - -) in CH_2Cl_2 at 298 K.

ligands, in which the energy follows the order **1** ≈ **2** ≈ **3** > **5** ≈ **6**, consistent with the better π-accepting abilities of the diynyl ligands than the monoynyl ligands. With reference to the previous spectroscopic works on platinum(II)−alkynyl systems[5] and related work on $(Bu_4N)_2[Pt(C{\equiv}CC_6H_5)_4]$,[18b] as well as the observed trend in absorption energies, the higher energy bands for **1**−**3**, **5**, and **6** are ascribed to the intraligand (IL) $\pi \rightarrow \pi^*$ transitions of the alkynyl ligands, while the low-energy absorptions are tentatively assigned as [d(Pt) → π^*(C≡CR)] metal-to-ligand charge transfer (MLCT) transitions, with some mixing of an intraligand (IL) $\pi \rightarrow \pi^*$(C≡CR) transition. The electronic absorption spectrum of complex **7** also shows a pattern similar to that of its precursor complex **6**, with the lowest energy absorption band shifted from 388 nm in **6** to 434 nm in **7**. With reference to previous studies on $[Pt_2Ag_4(C{\equiv}CC_6H_5)_8]$,[18a] the low-energy absorption may be tentatively assigned as an alkynyl-to-metal cluster core ligand-to-metal charge transfer (LMCT) [RC≡CC≡C$^-$ → Pt_2M_4] transition, probably mixed with some intraligand alkynyl character. Alternatively, the transition may be viewed as a $[Pt(C{\equiv}C{-}C{\equiv}CR)_4]^{2-}$ to Pt_2M_4 metalloligand-to-metal cluster core transition. The red shift in the low-energy band from its analogue complex $[Pt_2Ag_4(C{\equiv}CC_6H_5)_8]$[18] at 394 nm to 434 nm in **7** is consistent with such an assignment as the better π-donor ability of the diynyl ligand than the monoynyl ligand would give rise to a higher-lying π(C≡C−C≡CR) orbital energy, leading to a lower transition energy in **7**.

The electronic absorption spectrum of the 4-ethynylpyridine-bridged dinuclear platinum(II) complex, $[Pt(^tBu_3trpy)(C{\equiv}CC_5H_4N)Pt(^tBu_3trpy)](PF_6)_3$ (**4**), shows vibronic-structured bands at 288−360 nm, characteristic of the intraligand (IL) transition of the terpyridine ligand. Besides the IL transitions, a low-energy shoulder at 400 nm is observed. With reference to previous spectroscopic studies on platinum(II)−terpyridyl,[7e−g] this low-energy band at 400 nm is assigned as the d_π(Pt) → π^*(trpy) metal-to-ligand charge transfer (MLCT) transition.

Complexes **1**−**6** all show emission properties in the solid state and in solutions both at room temperature and at 77 K, while complex **7** is nonemissive in the solid state at room temperature. The luminescence quantum yields of the complexes in dichloromethane are found to be on the order of 10^{-2}−10^{-1}. The emission data of complexes **1**−**7** are shown in Table 3. Representative emission spectra of these complexes are illustrated in Figures 4 and 5. The emission spectra of **1**−**3** are rich in vibronic structures with vibrational progressional spacings of ca. 2000−2200 cm^{-1}, typical of the ν(C≡C) stretch, and ca. 1200−1400 cm^{-1}, typical of the ν(C···C) and ν(C···N) modes of the pyridyl units. Complex **3** was found to show a slightly lower energy emission relative to complexes **1** and **2** both in solution and in 77 K glass. A red shift in the emission energy is observed for complexes **5** and **6** relative to **1**−**3**. With reference to our earlier work on platinum(II)−alkynyl systems[5] and the previous work on $(Bu_4N)_2[Pt(C{\equiv}CC_6H_5)_4]$,[5b] the origin of the luminescence is assigned as derived from states of a [d(Pt) → π^*(C≡CR)] metal-to-ligand charge transfer (MLCT) character, mixed with intraligand (IL) $\pi \rightarrow \pi^*$(C≡CR) character. Such an assignment is also in line with the red shift observed upon changing the ligand from ethynylpyridine to ethynylpyrimidine and from monoynyl to the diynyl units, as a result of the lower π^* orbital energy of ethynylpyrimidine than ethynylpyridine and of the diynyl than the monoynyl unit. For complex **7**, it is likely that the low-energy emission at ca. 542−588 nm, which is absent in the mononuclear $[Pt(C{\equiv}C{-}C{\equiv}CR)_4]^{2-}$ complexes, is characteristic of the polynuclear mixed-metal alkynyl core. With reference to previous spectroscopic works on a related series of $[Pt_2Ag_4(C{\equiv}CR)_8]$,[18a] in which a ligand to metal−metal charge transfer (LMMCT) origin has been suggested on the basis of the finding that a shift in the emission energy to the red was observed upon going from R = C_6H_5 to R = C_6H_4OMe, the emission of **7** is similarly assigned as derived from a LMMCT origin. Alternatively, one can view the emission as a $[Pt(C{\equiv}C{-}C{\equiv}CR)_4]^{2-}$ → Ag_4Pt_2 metalloligand-to-cluster-centered emission. However, one could not exclude the possibility of some mixing of intraligand (IL) character into the excited state. One should be aware that the assignments of electronic transitions between metal and/or ligand localized orbitals are only rough approximations because of the possible extensive orbital mixing in these complexes. In addition, the emission lifetime in the microsecond range is suggestive of a triplet origin. The red shift in the low-energy band from its analogue complex, $[Pt_2Ag_4(C{\equiv}CC_6H_5)_8]$, is consistent with such an assignment as the better π-donor ability of the diynyl ligand than the monoynyl ligand would give rise to a higher-lying π(C≡C−C≡CR) orbital energy, leading to a lower transition energy in **7**.

Upon excitation at λ > 400 nm, **4** exhibits intense luminescence at ca. 505−615 nm both in solid state and in solution. With reference to the spectroscopic studies on other platinum(II)−terpyridyl systems,[7] the origin of the lowest energy excited state is assigned as derived from states of predominantly ^{3}MLCT [d_π[Pt(alkynyl)] → $\pi^*(^tBu_3trpy)$] character, probably mixed with some intraligand ^{3}IL [$\pi \rightarrow \pi^*$(C≡C)] and ligand-to-ligand charge transfer ^{3}LLCT [π(C≡C) → $\pi^*(^tBu_3trpy)$] character. It is likely that the Pt center attached to the alkynyl unit is more electron-rich than the Pt center attached to the pyridyl moiety, given the better electron-donating ability and the anionic nature of the alkynyl ligand. Figure 6 depicts the excitation and emission spectra of **4**. The excitation band at ca. 405 nm, which closely

Table 3. Electronic Absorption and Emission Data of **1**−**7**

complex	absorption[a] λ/nm (ϵ_{max}/dm^3 mol^{-1} cm^{-1})	emission medium (T/K)	λ_{em}/nm (τ_0/μs)	quantum yield,[b] ϕ_{em}
1	305 (55 550), 348 (46 090)	solid (298)	462[c] (0.5 ± 0.1)	0.035
		solid (77)	460[c] (1.3 ± 0.1)	
		CH_2Cl_2 (298)	450[c] (0.2 ± 0.1)	
		glass[a](77)	442[c] (14.1 ± 0.1)	
2	290 (41 710), 342 (42 100)	solid (298)	469[c] (1.6 ± 0.1)	0.051
		solid (77)	470[c] (3.8 ± 0.1)	
		CH_2Cl_2 (298)	460[c] (0.2 ± 0.1)	
		glass[a](77)	454[c] (21.6 ± 0.1)	
3	290 (48 330), 345 (28 920)	solid (298)	468[d] (2.2 ± 0.1)	0.044
		solid (77)	472[d] (4.8 ± 0.1)	
		CH_2Cl_2 (298)	475[d] (1.8 ± 0.1)	
		glass[a] (77)	467[d] (28.2 ± 0.1)	
4	288 (56 380), 308 (56 030),	solid (298)	580 (0.6 ± 0.1)	0.121
	322 (40 220), 338 (38 570),	solid (77)	590 (1.5 ±0.1)	
	400 (10 950)	CH_2Cl_2 (298)	505 (0.7 ± 0.1)	
		glass[a] (77)	610 (3.8 ± 0.1)	
5	276 (57 250), 310 (68 150), 322 (69 570), 360 (108 640),	solid (298)	542[c] (4.0± 0.1)	0.043
	390 (13 340)	solid (77)	537[c] (19.0 ± 0.1)	
		CH_2Cl_2 (298)	490[c] (4.0 ± 0.1)	
		glass[a] (77)	485[c] (24.7 ± 0.1)	
6	276 (52 690), 310 (61 250), 322 (62 680), 360 (93 310),	solid (298)	541[c] (7.5 ± 0.1)	0.046
	388 (15 070)	solid (77)	535[c] (13.0 ± 0.1)	
		CH_2Cl_2 (298)	490[c] (6.4 ± 0.1)	
		glass[a] (77)	489[c] (21.6 ± 0.1)	
7	290 (89 640), 308 (77 630),	solid (298)	*e* (590[f])	0.009
	334 (34 930), 364 (17 070),	solid (77)	588 (1.5 ± 0.1)	
	434 (41 040)	CH_2Cl_2 (298)	562 (2.1 ± 0.1)	
		glass[a] (77)	542[c] (7.8 ± 0.1)	

[a] In EtOH−MeOH (4:1 v/v). [b] The quantum yield was measured at room temperature with quinine sulfate as a standard. From ref 12. [c] Vibronic-structured with vibrational progressional spacings of 1900−2150 cm^{-1}. [d] Vibronic-structured with vibrational progressional spacings of 1200−1400 cm^{-1}. [e] Not emissive. [f] In crystal form before rigorous drying.

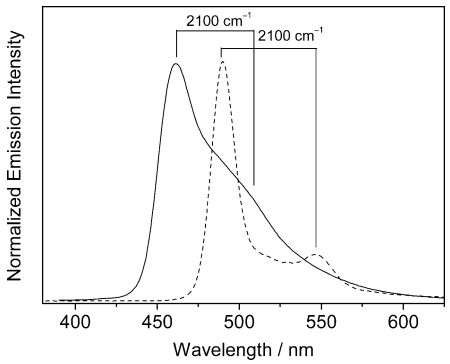

Figure 4. Normalized emission spectra of $(Bu_4N)_2[Pt(C{\equiv}CC_5H_4N\text{-}3)_4]$ (**2**) (—) and $(Bu_4N)_2[Pt(C{\equiv}CC{\equiv}CC_5H_5)_4]$ (**5**) (- - -) in CH_2Cl_2 at 298 K.

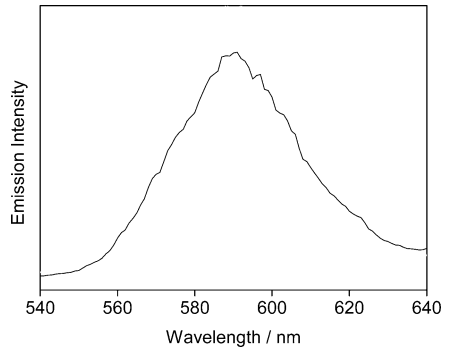

Figure 5. Emission spectrum of $[Pt_2Ag_4(C{\equiv}CC{\equiv}CC_6H_4CH_3\text{-}4)_8(THF)_4]$ (**7**) in CH_2Cl_2 at 298 K.

matches that of the low-energy MLCT band in the electronic absorption spectrum, further supports the assignment of the emission origin as a ^{3}MLCT state, mixed with some ^{3}IL/^{3}-LLCT character.

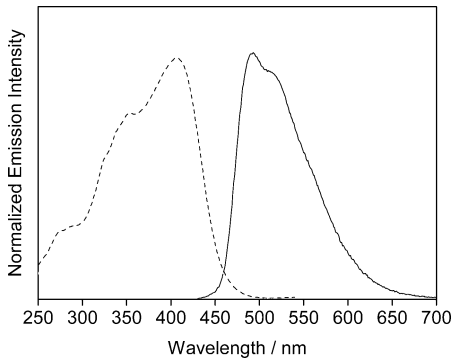

Figure 6. Normalized emission (—) and excitation (- - -) spectra of $[Pt(^tBu_3trpy)(C{\equiv}CC_5H_4N)Pt(^tBu_3trpy)](PF_6)_3$ (**4**) in CH_2Cl_2 at 298 K.

The electrochemical properties of complexes **1**−**7** have been investigated by cyclic voltammetry and the electrochemical data in acetonitrile (0.1 mol dm^{-3} ^{n}Bu$_4$NPF$_6$) are summarized in Table 4. The representative cyclic voltammograms for the oxidative scans of complexes **1**−**3** and **5**−**7** show one irreversible oxidation wave at ca. +0.71 to +1.00 V, with no observable reduction waves even upon scanning to ca. −2.0 V vs SCE. On the contrary, complex **4** shows only four reduction couples with no oxidation waves observed upon scanning to +2.0 V SCE (Figure 7). With reference to previous studies on platinum(II)−alkynyl complexes,[23] the irreversible anodic wave at ca. +0.69 to +0.86 V in **1**−**3**, **5**, and **6** is tentatively assigned as platinum metal-centered Pt(II) → Pt(III) oxidation. The irreversible nature of the oxidation wave is suggestive of the instability of the one-electron oxidized form, which decomposes readily in solution within the time scale of the cyclic voltammetric experiment. A close resemblance of the potential of the

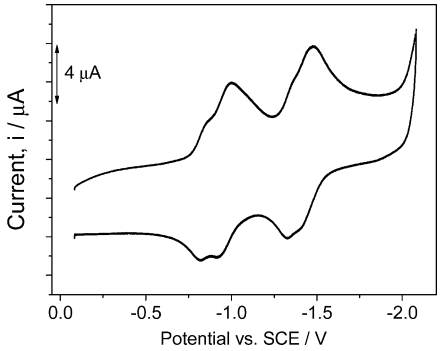

Figure 7. Cyclic voltammogram of [Pt(^{t}Bu$_3$trpy)(C≡CC$_5$H$_4$N)Pt(^{t}Bu$_3$trpy)](PF$_6$)$_3$ (**4**) in MeCN (0.1 M ^{n}Bu$_4$NPF$_6$) showing the reductive scan.

Table 4. Electrochemical Data for **1**−**7** in Acetonitrile Solution (0.1 M ^{n}Bu$_4$NPF$_6$) at 298 K[a]

complex	oxidation E_{pa}[b]/V vs SCE	reduction $E_{1/2}$[c]/V vs SCE
1	+0.72	
2	+0.71	
3	+0.72	
4		−0.82, −0.93, −1.33, −1.42
5	+0.88	
6	+0.80	
7	+1.00	

[a] Working electrode, glassy carbon; scan rate 100 mV s^{-1}. [b] E_{pa} is the peak anodic potential of the irreversible oxidation wave. [c] $E_{1/2} = (E_{pa} + E_{pc})/2$; E_{pa} and E_{pc} are peak anodic and peak cathodic potentials, respectively.

irreversible oxidation waves for **1**−**3** as well as the more positive potential for **5** and **6** than for **1**−**3**, with trends in the order **1** (+0.72 V) ≈ **2** (+0.71 V) ≈ **3** (+0.72 V) < **6** (+0.80 V) < **5** (+0.88 V), is attributed to an increase in the π-accepting ability of the alkynyl ligands upon going from the monoynyl to the diynyl unit, which would render the d_π(Pt) orbital more low-lying in energy, rendering the metal-centered oxidation more difficult in the diynyl complexes. Similarly, the more positive potential for **5** than for **6** can be rationalized by the presence of electron-donating methyl groups on the alkynyl ligands in **6**, resulting in a less π-accepting alkynyl and thus rendering the metal-centered oxidation more readily to occur. For complex **7**, with reference to the monoynyl analogue [Pt$_2$Ag$_4$(C≡CPh)$_8$][18a] as well as the previous studies on heterometallic Pt−M (M = Cu, Ag) alkynyl systems,[23] such as [Pt(P^P)$_2$(C≡CR)$_2$-{M(MeCN)$_2$}$_2$](PF$_6$)$_2$ (P^P = dppy, dppm; R = Ph, SiMe$_3$, ^{t}Bu; M = Cu, Ag)[23b,c] which suggest that the d^{10} metal centers (Cu^I or Ag^I) are more readily oxidized and reduced than the Pt(II) center, the irreversible oxidation couple at ca. +1.00 is tentatively ascribed to a Ag^I metal-centered oxidation. However, the possibility of an assignment of the oxidation wave as a Pt^{II} metal-centered Pt(II) → Pt(III) oxidation may not be excluded. The cyclic voltammogram of complex **4** shows four quasi-reversible reduction couples with two at ca. −0.82 to −0.93 vs SCE and two at ca. −1.33 to −1.42 V vs SCE. With reference to previous studies on the related platinum terpyridyl systems,[24] the reduction couples are tentatively assigned as terpyridyl-based reductions with some mixing of Pt(II) metal character. The two sets of couples are believed to correspond to the successive one-electron reductions of the two terpyridine moieties.

Acknowledgment. V.W.-W.Y. acknowledges support from The University of Hong Kong Foundation for Educational Development and Research Limited and the receipt of a Croucher Senior Research Fellowship from the Croucher Foundation. The work described in this paper has been supported by a CERG grant from the Research Grant Council of the Hong Kong Special Administrative Region, People's Republic of China (Project HKU7123/00P). C.-K.H. acknowledges the receipt of a postgraduate studentship, and N.Z., the receipt of a university postdoctoral fellowship, both administered by The University of Hong Kong.

Supporting Information Available: Tables of atomic coordinates, thermal parameters, and a full list of bond distances and angles for **4** and **7** in PDF format, and crystallographic data in CIF format. This material is available free of charge via the Internet at http://pubs.acs.org.

IC034877L

(23) Yam, V. W. W.; Chan, L. P.; Lai, T. F. *J. Chem. Soc., Dalton Trans.* **1993**, 2075−2079.
(24) (a) Crites, D. K.; Cunningham, C. T.; McMillin, D. R. *Inorg. Chim. Acta*. **1998**, *273*, 346−353. (b) Hill, M. G.; Bailey, J. A.; Miskowski, V. M.; Gray, H. B. *Inorg. Chem.* **1996**, *35*, 4585−4590.